IOP Conf. Series: Materials Science and Engineering **10** (2010) 012165 doi:10.1088/1757-899X/10/1/012165

POD-based model order reduction for the simulation of strong nonlinear evolutions in structures: application to damage propagation

P. Kerfriden, P. Gosselet [1], S. Adhikari [2], S. Bordas [3], J.-C. Passieux

Cardiff University, Queen's Buildings, The Parade, Cardiff CF24 3AA, Wales, UK
ENS Cachan, 61 Avenue du Président Wilson, F-94230 Cachan, France
Swansea University, Singleton Park, Swansea, SA2 8PP, Wales UK
Cardiff University, Queen's Buildings, The Parade, Cardiff CF24 3AA, Wales, UK
INSA Lyon, 27, avenue Jean Capelle, 69621 Villeurbanne, France

E-mail: kerfridenp@cardiff.ac.uk

Abstract. In this paper, we develop a bridge between POD-based model order reduction techniques and the classical Newton-Krylov solvers to derive an efficient solution procedure for highly nonlinear problems undergoing strong topological changes.

1. Introduction

During the last decades, the simulation of failure in complex materials has been one important issue in mechanical engineering. Micro and meso-scale models have demonstrated their ability to predict complex phenomena such as crack initiation and propagation in various fields: composite materials in aeronautics [14, 17], cement-based structures [10] in civil engineering or biostructures [8] in medical engineering. However, these models usually describe the material at a very fine scale compared to the size of the structure, and the finite element discretization of the underlying partial differential equations leads to large, potentially highly nonlinear (therefore requiring a fine discretization in time), numerical problems. Various multiscale computational strategies have been developed to tackle this important issue, such as enrichment techniques [3], homogenization techniques [7, 6], multiscale domain decomposition strategies [9, 13], or model order reduction[11, 16]. The most efficient of these techniques couple several of these features [20, 12, 13, 4, 24].

Among them, Proper Orthogonal Decomposition-based (POD) [11, 16, 15] model order reduction strategies provide extremely valuable tools for an automatic derivation of a multiscale computational method (no *a priori* physical understanding of the different scales involved is required). They basically consist in using a set of potential solutions to the initial problem (snapshot) and extracting, by a spectral analysis a few basis vectors spanning a space of small dimension in which the solution to the initially large numerical problem is well approximated [25]. They techniques have been proved extremely efficient when speed is more important

[1] CNRS Research Associate
[2] Chair of Aerospace Engineering
[3] Royal Academy of Engineering/Leverhulme Senior Research Fellowship

that accuracry, for instance if the goal simulation is to provide an approximative response of a complex structure in real-time (a example of biomedical application is given in [19]). This type of applications is our main focus.

In the context of structural problems involving plasticity or damage, two severe drawbacks limit the direct application of this method:

- strong topological changes in the structure might occur, and the initial snapshot might be too poor to represent accurately the solution of the damaged structure. Improvements have been proposed by Ryckelynk's team [22] where the reduced basis is enriched during the computation. When required, a Krylov subspace associated to a linearized operator of the initial problem is generated, and a few additional basis vectors are obtained by a spectral analysis of this space. However, it seems that, when dealing with complex constitutive laws, this adaptive strategy can be computationally expensive [24].
- the integration of the constitutive law needs to be done at each integration point, regardless of the dimension of the reduced space. These problems have been handled in [23] by a technique called hyperreduction, which consists in considering only a few local residuals to compute the internal forces.

On the other hand, various model order reduction strategies have also been used to derive good initializations and preconditioners for iterative algorithms for complex nonlinear problems at the fine scale [18, 21, 9, 20, 12].

We propose here a new way to couple these two approaches. Our vision is that if complex changes in the topology of the structure appear (local crack initiation for instance), they can only be accurately predicted by solving the fine scale model, at least locally. This can be done, for instance, by adding the finite element shape functions to the snapshot, or by using relocalization techniques. However, the long-range effects of these topological changes do not require the fine description, and can be obtained by solving the full system in very crudely. Hence, when the global residual exceeds a given threshold value, we propose to perform conjugate gradient (CG) iterations on the full system, orthogonally to the snapshot space by means of a classical projection (this threshold value is thus the main parameter of the proposed strategy). The new vector obtained by the CG does not belong to the initial approximation space and is added to the reduced basis. It is interpreted as an "on-the-fly" enrichment of the reduced model.

This strategy can be interpreted as a bridge between exact Newton-Krylov strategies, and the POD method for nonlinear problems. Indeed, setting the residual threshold to a low value leads to the former strategy, while setting it to a high value leads to the latter. An intermediate value yields an adaptive model order reduction method with control of the global residual.

The paper is organized as follows. In Section 2, the nonlinear system of equations resulting from the discretization of a continuum mechanics problem is derived. The solution procedure applied at each time increment is described. The basic model order reduction is introduced in Section 3, and issues concerning the reduction of damage evolution simulations by the basic POD are discussed in Section 4. In section 5, we propose the POD-Krylov projection strategy, analyse the influence of its parameters in Section 6, and eventually give some results in Section 7.

2. Problem statement and basic solution strategy

2.1. Nonlinear structural Problem

Let us consider a structure occupying a continuous Domain Ω of boundary $\partial\Omega$. This structure is subjected to prescribed displacements $\underline{U}_{\mathrm{D}}$ on its boundary $\partial\Omega_u$, over Time interval [0 T]. Let $\underline{u}$ be the unknown displacement field, it belongs to the space $\mathcal{U}$ of kinematically admissible fields:

$$\mathcal{U} = \left\{ \underline{u} \in H^1(\Omega) / \underline{u}_{|\partial\Omega_u} = \underline{U}_{\mathrm{D}} \right\} \tag{1}$$

Let $\mathcal{U}_0$ be the associated vector space. Prescribed tractions $\underline{F}_{\mathrm{D}}$ are applied on the complementary boundary $\partial\Omega_f = \partial\Omega \backslash \partial\Omega_u$. Under the assumptions of quasi-static evolution of the structure and small perturbations, the weak form of the equilibrium reads, at any time $t \in [0\ T]$:

$$\begin{aligned} &\forall \underline{u}^\star \in \mathcal{U}_0,\ \textit{find } \underline{u} \in \mathcal{U} \textit{ such that:} \\ &\int_\Omega \underline{\underline{\sigma}} : \underline{\underline{\epsilon}}(\underline{u}^\star)\ d\Omega = \int_\Omega \underline{f}_{\mathrm{D}}.\underline{u}^\star\ d\Omega + \int_{\partial\Omega_f} \underline{F}_{\mathrm{D}}.\underline{u}^\star\ d\Gamma \end{aligned} \tag{2}$$

where $\underline{\underline{\sigma}}$ is the Cauchy stress tensor and $\underline{\underline{\epsilon}}(\underline{u})$ is the symmetric part of the gradient of displacement.

The constitutive relation between $\underline{\underline{\sigma}}$ and $\underline{\underline{\epsilon}}(\underline{u})$ is nonlinear and described using internal variables (for instance damage or plasticity). It is assumed to be local and rate-independent; it writes at Time t:

$$\underline{\underline{\sigma}} = \underline{\underline{\sigma}}\left(\left(\underline{\underline{\epsilon}}(\underline{u})_{|\tau}\right)_{\tau \leq t}\right) \tag{3}$$

2.2. Finite element space discretization

We perform a standard finite element approximation of the displacement fields described previsouly. The introduction of the finite element approximation into Equations (1), (2) and (3) leads to the following nonlinear vectorial equation at any time $t \in [0\ T]$:

$$\underline{\mathbf{F}}_{\mathrm{Int}}\left(\left(\underline{\mathbf{U}}_{|\tau}\right)_{\tau \leq t}\right) + \underline{\mathbf{F}}_{\mathrm{Ext}} = 0 \tag{4}$$

where $\underline{\mathbf{U}} \in \mathbb{R}^{n_n}$ (n_n is the number of nodal unknowns) is the vector of nodal displacement unknowns, $\underline{\mathbf{F}}_{\mathrm{Int}} \in \mathbb{R}^{n_n}$ and $\underline{\mathbf{F}}_{\mathrm{Ext}} \in \mathbb{R}^{n_n}$ are respectively the internal forces resulting from the discretization of the internal virtual work (left-hand side of (2)) and the external forces resulting from the discretization of the external virtual work (right-hand side of (2)) .

2.3. Time discretization

The nonlinear solution strategy used here is a classical time discretization scheme for quasi-static and rate-independant problems. The constitutive law being rate independent and the inertia effects being neglected, this procedure consists in finding a set of consecutive solutions at Times $(t_n)_{n \in [\![0\ n_t]\!]}$ (see [2]). Hence, the constitutive law (3) is discrete in Time. This time discretization scheme finally yields the following vectorial system of nonlinear equations at Time t_n:

$$\underline{\mathbf{F}}_{\mathrm{Int}}\left(\left(\underline{\mathbf{U}}_{|t_m}\right)_{m \in [\![0\ n]\!]}\right) + \underline{\mathbf{F}}_{\mathrm{Ext}} = 0 \tag{5}$$

For the sake of clarity, the dependency of the internal forces with the history of the solution fields will not be written explicitly.

2.4. Nonlinear solution strategy

At each time $(t_n)_{n \in [\![0\ n_t]\!]}$, the nonlinear problem is solved by a Newton-Raphson algorithm. At any iteration $(i+1)$ of the algorithm, a linear prediction is performed:

$$\underline{\underline{\mathbf{K}}}^i_{\mathrm{T}}\, \underline{\mathbf{\Delta U}}^{i+1} = \underline{\mathbf{R}}^i \tag{6}$$

where we have introduced the residual vector $\underline{\mathbf{R}} = \underline{\mathbf{F}}_{\mathrm{Ext}} + \underline{\mathbf{F}}_{\mathrm{Int}}(\underline{\mathbf{U}})$, and the increment of displacement $\underline{\mathbf{\Delta U}}^{i+1} = \underline{\mathbf{U}}^{i+1} - \underline{\mathbf{U}}^i$. This linear prediction is followed by a correction stage:

$$\underline{\mathbf{R}}^{i+1} = \underline{\mathbf{F}}_{\mathrm{Ext}} + \underline{\mathbf{F}}_{\mathrm{Int}}(\underline{\mathbf{U}}^{i+1}) \qquad \underline{\underline{\mathbf{K}}}^{i+1}_{\mathrm{T}} = \left.\frac{\partial \underline{\mathbf{F}}_{\mathrm{Int}}(\underline{\mathbf{U}})}{\partial \underline{\mathbf{U}}}\right|_{\underline{\mathbf{U}}=\underline{\mathbf{U}}^{i+1}} \tag{7}$$

3. Model order reduction

The set of equations (5) can be huge if multiscale problems are simulated (see for instance [3, 12]). Various strategies can be applied to reduce the size of this system without loosing accuracy. We apply here the classical model order reduction by projection to the resolution of problem (5).

3.1. Reduction by projection

The solution vector is searched for in a space of small dimension (several orders smaller than the number of finite element degrees of freedom). Let us call $\underline{\underline{\mathbf{C}}}$ the matrix whose columns form a basis of this space:

$$\underline{\underline{\mathbf{C}}} = \left(\begin{array}{cccc} \underline{\mathbf{C}}^1 & \underline{\mathbf{C}}^2 & \ldots & \underline{\mathbf{C}}^{n_C} \end{array} \right) \tag{8}$$

where n_C is the dimension of the reduced space, and $(\underline{\mathbf{C}}^k)_{k\in[\![1\ n_C]\!]} \in (\mathbb{R}^{n_n})^{n_C}$ are the chosen basis vectors. Applied to the reduction of Problem (5), the solution field is searched for under the form $\underline{\mathbf{U}} = \underline{\underline{\mathbf{C}}}\,\underline{\boldsymbol{\alpha}}$. The residual of Equation (5) is constrained to be orthogonal to a space of small dimension, which can, in theory, be different from the one spanned by $(\underline{\mathbf{C}}^k)_{k\in[\![1\ n_C]\!]}$. Let us limit our study to the Galerkin procedure, which writes the following constraint: $\underline{\underline{\mathbf{C}}}^T\,\underline{\mathbf{R}} = 0$ Hence, the reduced form of Problem (5) reads:

$$\underline{\underline{\mathbf{C}}}^T(\underline{\mathbf{F}}_{\text{Ext}} + \underline{\mathbf{F}}_{\text{Int}}(\underline{\underline{\mathbf{C}}}\,\underline{\boldsymbol{\alpha}})) = 0 \tag{9}$$

3.2. Solution procedure for the reduced nonlinear problem

At each time step of the time discretization scheme, the reduced problem (9) is solved by a Newton-Raphson algorithm. The $(i+1)^{th}$ prediction stage is performed using the following linearized equation:

$$\underline{\underline{\mathbf{K}}}^i_{\text{T,R}}\,\underline{\boldsymbol{\Delta\alpha}}^{i+1} = \underline{\mathbf{R}}^i_R \tag{10}$$

where the residual of the reduced nonlinear problem (9) is defined by $\underline{\mathbf{R}}_R = \underline{\underline{\mathbf{C}}}^T\,\underline{\mathbf{F}}_{\text{Ext}} + \underline{\underline{\mathbf{C}}}^T\,\underline{\mathbf{F}}_{\text{Int}}(\underline{\underline{\mathbf{C}}}\,\underline{\boldsymbol{\alpha}})$ and the increment $\underline{\boldsymbol{\Delta\alpha}}^{i+1} = \underline{\boldsymbol{\alpha}}^{i+1} - \underline{\boldsymbol{\alpha}}^i$. The correction stage reads:

$$\underline{\mathbf{R}}^{i+1}_R = \underline{\underline{\mathbf{C}}}^T\,\underline{\mathbf{F}}_{\text{Ext}} + \underline{\underline{\mathbf{C}}}^T\,\underline{\mathbf{F}}_{\text{Int}}(\underline{\underline{\mathbf{C}}}\,\underline{\boldsymbol{\alpha}}^{i+1}) \qquad\qquad \underline{\underline{\mathbf{K}}}^{i+1}_{\text{T,R}} = \underline{\underline{\mathbf{C}}}^T\,\left.\frac{\partial \underline{\mathbf{F}}_{\text{Int}}(\underline{\underline{\mathbf{C}}}\,\underline{\boldsymbol{\alpha}})}{\partial \underline{\boldsymbol{\alpha}}}\right|_{\underline{\boldsymbol{\alpha}}=\underline{\boldsymbol{\alpha}}^{i+1}} \tag{11}$$

Remark: there is a simple link between the previous solution procedure for the reduced problem (9) *and the systematic reduction of the prediction stages performed on the full nonlinear problem* (6) *since* $\underline{\underline{\mathbf{K}}}^i_{T,R}$ *can be expanded as*

$$\underline{\underline{\mathbf{K}}}^i_{T,R} = \underline{\underline{\mathbf{C}}}^T\,\left.\frac{\partial \underline{\mathbf{F}}_{Int}(\underline{\underline{\mathbf{C}}}\,\underline{\boldsymbol{\alpha}})}{\partial \underline{\boldsymbol{\alpha}}}\right|_{\underline{\boldsymbol{\alpha}}=\underline{\boldsymbol{\alpha}}^i} = \underline{\underline{\mathbf{C}}}^T\,\left.\frac{\partial \underline{\mathbf{F}}_{Int}(\underline{\mathbf{U}})}{\partial \underline{\mathbf{U}}}\right|_{\underline{\mathbf{U}}=\underline{\underline{\mathbf{C}}}\,\underline{\boldsymbol{\alpha}}^i}\,\left.\frac{\partial \underline{\mathbf{U}}}{\partial \underline{\boldsymbol{\alpha}}}\right|_{\underline{\boldsymbol{\alpha}}=\underline{\boldsymbol{\alpha}}^i} = \underline{\underline{\mathbf{C}}}^T\,\underline{\underline{\mathbf{K}}}^i_T\underline{\underline{\mathbf{C}}} \tag{12}$$

This result can be injected in Equation (10)*, which yields:*

$$\underline{\underline{\mathbf{C}}}^T(\underline{\mathbf{R}}^i - \underline{\underline{\mathbf{K}}}^i_T\underline{\underline{\mathbf{C}}}\,\underline{\boldsymbol{\Delta\alpha}}^{i+1}) = 0 \tag{13}$$

This last equation is a simple reduction by projection of the $(i+1)^{th}$ *linear prediction of the Newton-Raphson scheme* (6) *used to solve the initial problem* (5)*. In other words, the prediction stage of any Newton iteration performed on the reduced problem yields exactly the same solution as a reduction of the linear prediction stage used to solve the initial problem.*

3.3. POD-like reduced approximation space

The snapshot-POD is a projection-based model order reduction technique which requires the knowledge of a representative family of solutions to the global problem. This set of vectors is called $(\underline{\mathbf{S}}^k)_{k\in[\![1\ n_S]\!]}$ and form an operator $\underline{\underline{\mathbf{S}}} = \left(\begin{array}{cccc} \underline{\mathbf{S}}^1 & \underline{\mathbf{S}}^2 & ... & \underline{\mathbf{S}}^{n_S} \end{array}\right)$. The aim is to find the family $(\underline{\mathbf{C}}^k)_{k\in[\![1\ n_C]\!]}$, of dimension n_C smaller than n_S such that the distance between spaces $\mathrm{Im}(\mathbf{C})$ and $\mathrm{Im}(\underline{\underline{\mathbf{S}}})$ is minimum (in the sense of the Frobenius norm).

This problem is classically solved by computing the singular value decomposition of $\underline{\underline{\mathbf{S}}}$:

$$\underline{\underline{\mathbf{S}}} = \underline{\underline{\mathbf{U}}}\,\underline{\underline{\mathbf{\Sigma}}}\,\underline{\underline{\mathbf{V}}}^T = \sum_{k=1}^{n_S} \Sigma^k\, \underline{\mathbf{U}}^k\, \underline{\mathbf{V}}^{kT} \tag{14}$$

where the $n_S - n_C$ smallest singular values of $\underline{\underline{\mathbf{\Sigma}}}$ have been replaced by zeros to form $\underline{\underline{\widetilde{\mathbf{\Sigma}}}}$. where $\underline{\underline{\mathbf{U}}} = \left(\begin{array}{cccc} \underline{\mathbf{U}}^1 & \underline{\mathbf{U}}^2 & ... & \underline{\mathbf{U}}^{n_N} \end{array}\right)$ and $\underline{\underline{\mathbf{V}}} = \left(\begin{array}{cccc} \underline{\mathbf{V}}^1 & \underline{\mathbf{V}}^2 & ... & \underline{\mathbf{V}}^{n_S} \end{array}\right)$ are two orthonormal matrices of respective sizes n_N and n_S and the upper block of $\underline{\underline{\mathbf{\Sigma}}}$ is a diagonal matrix of positive entries $(\Sigma^k)_{k\in[\![1\ n_S]\!]}$ (singular values), ordered decreasingly (the lower block is a null matrix). One can show that the optimum reduced snapshot basis $(\underline{\mathbf{C}}^k)_{k\in[\![1\ n_C]\!]}$ is such that:

$$\underline{\underline{\mathbf{C}}} = \left(\begin{array}{cccc} \underline{\mathbf{U}}^1 & \underline{\mathbf{U}}^2 & ... & \underline{\mathbf{U}}^{n_C} \end{array}\right) \tag{15}$$

3.4. POD for the reduction of damage evolution problems

We focus on a very simple damageable lattice structure, made of bars under traction or compression, in which the solution displacement field $\underline{u}$ is supposed constant through the section, and linear along the length of the bar (i.e.: one linear finite element per bar). We use a very basic constitutive law, based on classical damage mechanics [14]. The lineic strain energy of each bar reads:

$$e_d = \frac{1}{2} E(1-d) S \epsilon^2 \tag{16}$$

where ϵ is the strain in the direction of the bar and d is a damage variable which ranges from 0 (undamaged material) to 1 (completely damaged material). Two state equations can be derived from the strain energy. the first one links the normal force N to the strain, while the second one links a thermodynamic force Y to the strain:

$$N = \frac{\partial e_d}{\partial \epsilon} = E(1-d)S\epsilon \qquad Y = -\frac{\partial e_d}{\partial d} = \frac{1}{2} E S \epsilon^2 \tag{17}$$

An evolution law is defined to link the damage variable to the thermodynamic force:

$$d = \min\left(1, \sup_{\tau \le t}\left(\alpha (Y_{|\tau})^\beta\right)\right) \tag{18}$$

The results presented in this paper are obtained with the following set of data. The section and Young's modulus are unitary. A single damage variable is introduced for each bar. The material parameters are $\beta = 0.5$ and $\alpha = \sqrt{2}$. Each vertical or horizontal bar has a unitary length.

The initial problem we want to solve is described on Figure (1). The load is applied on the top surface of the structure, in the y direction and at position $x = 9$. The damage state represented here (light gray corresponds to $d = 0$, while darker bars are damaged) is obtained in 60 time increments, each of which is converged to a very low level of error. This problem being unstable, a local arc-length procedure is combined to the Newton algorithm. As presented in [1, 12], we use a quasi-Newton approximation of the previsouly described tangent Newton-Raphson algorithm. The tangent operator at iteration $(i+1)$ is replaced by the stiffness matrix obtained by setting the internal variables to the values obtained after the i^{th} correction stage.

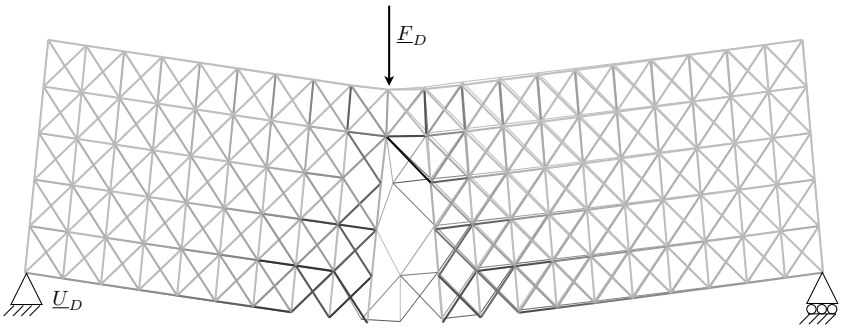

Figure 1. Reference solution (thin lines) and solution obtained with the enhanced projection algorithm (bold lines, $\nu_{\text{New}} = 4.0e^{-1}$)

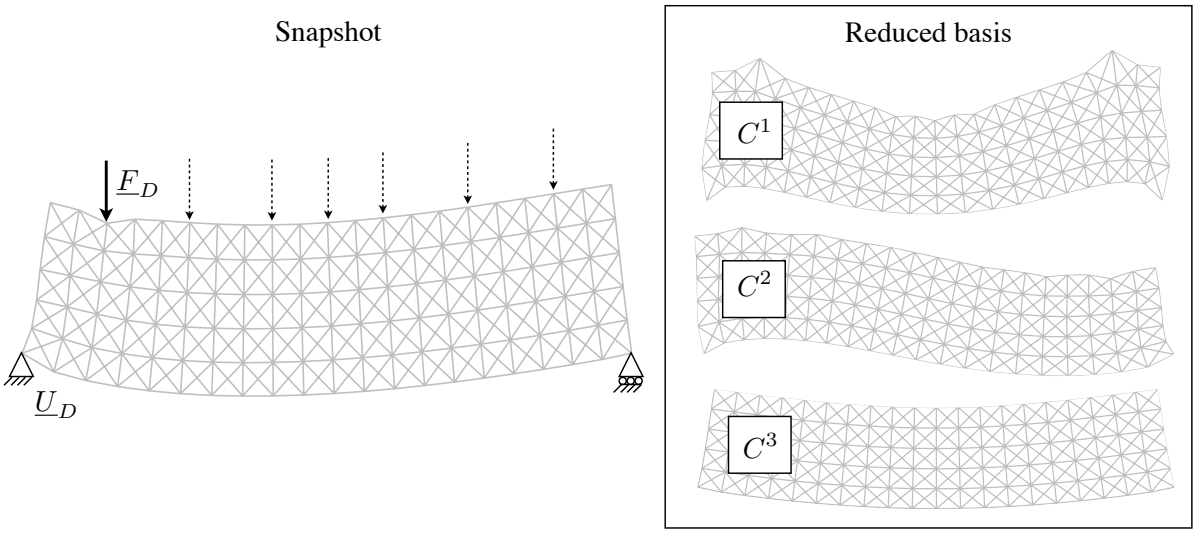

Figure 2. Snapshot computation (left), reduced snapshot (right)

In order to reduce this problem by a POD-based projection method, we compute a snapshot of 7 solutions (loads applied on the top surface of the lattice, at positions $x \in \{2\ 5\ 8\ 10\ 12\ 15\ 18\}$), as illustrated on Figure (2). The successive loads have a very low value, so that the structure is virtually undamaged. This snapshot is reduced to three basis vectors by the computation of a truncated SVD.

Given the normalized current solution $\underline{\widetilde{\mathbf{U}}}_{|t} = \frac{\underline{\mathbf{U}}_{|t}}{\|\underline{\mathbf{U}}_{|t}\|_2}$ and normalized reference solution $\underline{\widetilde{\mathbf{U}}}_{\text{ref}_{|t}} = \frac{\underline{\mathbf{U}}_{\text{ref}|t}}{\|\underline{\mathbf{U}}_{\text{ref}|t}\|_2}$, the solution error used to assess the accuracy of the current solution is:

$$\text{solution error}_{|t} = \left\| \underline{\widetilde{\mathbf{U}}}_{|t} - \underline{\widetilde{\mathbf{U}}}_{\text{ref}_{|t}} \right\|_2 \tag{19}$$

In the very early stages of the simulation, the error is very low (even if the application point of the force is not is the snapshot), which can be seen on Figure (3) (the dotted line is the error defined by Equation (19) as a function of time). However, as damage increases, which eventually leads to the crack represented on Figure (1), a simple linear combination of the modes of the reduced snapshot is obviously not sufficient to reproduce accurately the solution, which results in a high level of error.

4. POD-Krylov model order reduction

In order to handle complex changes in the topology of the structure, we propose to enrich the reduced basis $\mathbf{C}$, on-the-fly, during the Newton iterations performed on the reduced problem (9). Prior to the actual description of the algorithm, let us remark that, at each iteration of the Newton algorithm, one can compute:

- the relative norm of the residual of the reduced problem (9), i.e.: $\dfrac{\|\underline{\mathbf{R}}_R\|_2}{\|\underline{\underline{\mathbf{C}}}^T\underline{\mathbf{F}}_{\text{Ext}}\|_2}$
- the relative norm of the residual of the initial problem (5), i.e.: $\dfrac{\|\underline{\mathbf{R}}\|_2}{\|\underline{\mathbf{F}}_{\text{Ext}}\|_2}$

Our aim is to control both these values during the solution process. More precisely, we will proceed to the next time increment only if the former is lower than $\nu_{\text{New,R}}$ and the later lower than ν_{New}, with $\nu_{\text{New,R}} \ll \nu_{\text{New}}$. Typically, $\nu_{\text{New,R}}$ is set to $10e^{-6}$ in our tests, while the value of ν_{New} (which, in our tests, ranges from 10^{-1} to 8.10^{-1}) will determine the accuracy of the successive Newton resolutions, and is an important parameter of the strategy.

The following algorithm is applied. A sufficient number of Newton iterations are performed on the reduced problem, so that the norm of its residual is small enough (at least ten times smaller than the norm of the residual of the full problem). If the norm of the residual of the full problem is still higher than a desired value ν_{New}, the following linear prediction is enhanced by performing a few iterations of Conjugate Gradient on the linear prediction of the full problem (5). The resulting solution is eventually added to the reduced snapshot basis.

This process is repeated, until convergence of both the reduced problem ($\|\underline{\mathbf{R}}_R\|_2/\|\underline{\underline{\mathbf{C}}}^T\underline{\mathbf{F}}_{\text{Ext}}\|_2 \leq \nu_{\text{New,R}}$), and the full problem ($\|\underline{\mathbf{R}}\|_2/\|\underline{\mathbf{F}}_{\text{Ext}}\|_2 \leq \nu_{\text{New}}$).

4.1. Corrections on the linear predictions by an iterative solver

When required by the previously described algorithm, the enhanced linear prediction is performed by initializing a projected conjugate gradient and performing a few iterations on the linearized problem (6) (the stopping criterion on the normalized residual is denoted ν_{CG} and set to a high value, typically of the same order than ν_{New}). The reasons for this choice are the following:

- the construction of a Krylov basis requires only matrix/product operations (no matrix assembly or factorization). It is therefore very cheap when a very few iterations of the iterative solver are required, which, as demonstrated in the following examples, is our case. In addition, it is very suitable to parallel computing.
- the projection framework is an ideal tool for our particular problem. Indeed, the initialization of the projected algorithm is the linear prediction of the reduced problem, Equation (10). The complementary part of the solution is searched for is a space orthogonal to the reduced basis, which extends immediately the solution space and reduces the number of iterations required to reach ν_{CG} (left preconditioning). To summarize these ideas, each iteration of the CG is a correction of the solution to the reduced linear prediction (10) such that this correction is orthogonal to the initialization.

4.1.1. Projected Krylov solver The classical projected conjugate gradient [5] is applied to the approximate solution of (6) (assumed linear, symmetric, positive and definite), which is recalled here:

$$\underline{\underline{\mathbf{K}}}_{\text{T}}\,\underline{\boldsymbol{\Delta}\mathbf{U}} = \underline{\mathbf{R}} \tag{20}$$

Where the i superscripts have been dropped for the sake of clarity. The chosen augmentation space is the previously defined reduced snapshot space $\text{Im}(\underline{\underline{\mathbf{C}}})$.

The solution is searched for under the form:

$$\underline{\boldsymbol{\Delta \mathbf{U}}} = \underline{\boldsymbol{\Delta \mathbf{U}}}_{\mathrm{C}} + \underline{\boldsymbol{\Delta \mathbf{U}}}_{\mathrm{K}} \qquad \left\{ \begin{array}{c} \underline{\boldsymbol{\Delta \mathbf{U}}}_{\mathrm{C}} \in \mathrm{Im}(\underline{\underline{\mathbf{C}}}) \\ \underline{\boldsymbol{\Delta \mathbf{U}}}_{\mathrm{K}} \in \mathrm{Im}(\underline{\underline{\mathbf{C}}})^{\perp_{\underline{\underline{\mathbf{K}}}_{\mathrm{T}}}} = \mathrm{Ker}(\underline{\underline{\mathbf{C}}}^T \underline{\underline{\mathbf{K}}}_{\mathrm{T}}) \end{array} \right. \tag{21}$$

$\perp_{\underline{\underline{\mathbf{K}}}_{\mathrm{T}}}$ designing the $\underline{\underline{\mathbf{K}}}_{\mathrm{T}}-$orthogonality between the two supplementary spaces, which is ensured by introducing a projector $\underline{\underline{\mathbf{P}}}$ such that:

$$\underline{\boldsymbol{\Delta \mathbf{U}}}_{\mathrm{K}} = \underline{\underline{\mathbf{P}}}\, \widetilde{\underline{\boldsymbol{\Delta \mathbf{U}}}}_{\mathrm{K}} \qquad \underline{\underline{\mathbf{C}}}^T \underline{\underline{\mathbf{K}}}_{\mathrm{T}} \underline{\underline{\mathbf{P}}} = 0 \tag{22}$$

Hence, the decomposition of the increment of displacement reads:

$$\underline{\boldsymbol{\Delta \mathbf{U}}} = \underline{\underline{\mathbf{C}}}\, \underline{\boldsymbol{\Delta \alpha}} + \underline{\underline{\mathbf{P}}}\, \widetilde{\underline{\boldsymbol{\Delta \mathbf{U}}}}_{\mathrm{K}} \tag{23}$$

where the $\underline{\underline{\mathbf{K}}}_{\mathrm{T}}-$orthogonality is ensured by choosing $\underline{\underline{\mathbf{P}}} = \underline{\underline{\mathbf{I}}}_{\mathrm{d}} - \underline{\underline{\mathbf{C}}}(\underline{\underline{\mathbf{C}}}^T \underline{\underline{\mathbf{K}}}_{\mathrm{T}} \underline{\underline{\mathbf{C}}})^{-1} \underline{\underline{\mathbf{C}}}^T \underline{\underline{\mathbf{K}}}_{\mathrm{T}}$.

This separation of the search space into two subspaces $\mathrm{Im}(\underline{\underline{\mathbf{C}}})$ and $\mathrm{Im}(\underline{\underline{\mathbf{P}}})$ in direct sum leads to the following uncoupled equations:

$$(\underline{\underline{\mathbf{C}}}^T \underline{\underline{\mathbf{K}}}_{\mathrm{T}} \underline{\underline{\mathbf{C}}})\, \underline{\boldsymbol{\Delta \alpha}} = \underline{\underline{\mathbf{C}}}^T \underline{\mathbf{R}} \tag{24}$$

$$\left(\underline{\underline{\mathbf{P}}}^T \underline{\underline{\mathbf{K}}}_{\mathrm{T}} \underline{\underline{\mathbf{P}}}\right) \widetilde{\underline{\boldsymbol{\Delta \mathbf{U}}}}_{\mathrm{K}} = \underline{\underline{\mathbf{P}}}^T \underline{\mathbf{R}} \quad \Longleftrightarrow \quad \left(\underline{\underline{\mathbf{P}}}^T \underline{\underline{\mathbf{K}}}_{\mathrm{T}} \underline{\underline{\mathbf{P}}}\right) \underline{\boldsymbol{\Delta \mathbf{U}}}_{K} = \underline{\underline{\mathbf{P}}}^T \underline{\mathbf{R}}_{\mathrm{C}} \tag{25}$$

where $\underline{\mathbf{R}}_{\mathrm{C}} = \underline{\mathbf{R}} - \underline{\underline{\mathbf{K}}}_{\mathrm{T}}\, \underline{\boldsymbol{\Delta \mathbf{U}}}_{C}$. Equation (24) is a coarse initialization of the projected conjugate gradient. As stated previously, it is equivalent to the linear prediction of the reduced problem (Equation (10)). Equation (25) is the linear prediction of the full problem projected on $\mathrm{Im}(\underline{\underline{\mathbf{C}}})^{\perp_{\underline{\underline{\mathbf{K}}}_{\mathrm{T}}}}$. This system is symmetric and can be solved by a preconditionned conjugate gradient. Hence we solve:

$$\widetilde{\underline{\underline{\mathbf{M}}}}^{-1} \left(\underline{\underline{\mathbf{P}}}^T \underline{\underline{\mathbf{K}}}_{\mathrm{T}} \underline{\underline{\mathbf{P}}}\right) \underline{\boldsymbol{\Delta \mathbf{U}}}_{K} = \widetilde{\underline{\underline{\mathbf{M}}}}^{-1} \underline{\underline{\mathbf{P}}}^T \underline{\mathbf{R}}_{\mathrm{C}} \tag{26}$$

where $\widetilde{\underline{\underline{\mathbf{M}}}}^{-1}$ is a left preconditionner (symmetric, definite and positive). In our test cases, $\widetilde{\underline{\underline{\mathbf{M}}}}$ is diagonal matrix whose entries are the elements of the diagonal of $\underline{\underline{\mathbf{K}}}_{\mathrm{T}}$.

4.1.2. New augmentation At the end of each enhanced prediction step, the approximate solution vector to (6) is added to the approximation space $\mathrm{Im}(\underline{\underline{\mathbf{C}}})$.

$$\underline{\underline{\mathbf{C}}} = \left(\begin{array}{ccc} \underline{\underline{\mathbf{C}}}_{\mathrm{POD}} & \underline{\underline{\mathbf{C}}}_{\mathrm{CG,old}} & \underline{\underline{\mathbf{C}}}_{\mathrm{CG}} \end{array} \right) \tag{27}$$

$\underline{\underline{\mathbf{C}}}_{\mathrm{POD}}$ is the initial reduced snapshot (classical POD). $\underline{\underline{\mathbf{C}}}_{\mathrm{CG}}$ is the normalized solution vector $\underline{\mathbf{U}}^{i+1} = \underline{\boldsymbol{\Delta \mathbf{U}}}^{i+1} + \underline{\mathbf{U}}^{i}$ obtained during the last enhanced linear prediction ($(i+1)^{th}$ Newton iteration). $\underline{\underline{\mathbf{C}}}_{\mathrm{CG,old}}$ is the set of complementary parts obtained during the previous enhanced linear predictions. When the size of $\underline{\underline{\mathbf{C}}}_{\mathrm{CG,old}}$ exceeds a critical value, a SVD is performed on this matrix, as described previously to obtain the reduced snapshot $\underline{\underline{\mathbf{C}}}_{\mathrm{POD}}$.

Understanding the gain obtained by using $\underline{\underline{\mathbf{C}}}_{\mathrm{CG,old}}$ requires a deep parametric study which is not the subject of this paper. Instead, we demonstrate the efficiency of the following cheap enrichment $\underline{\underline{\mathbf{C}}} = \left(\begin{array}{cc} \underline{\underline{\mathbf{C}}}_{\mathrm{POD}} & \underline{\underline{\mathbf{C}}}_{\mathrm{CG}} \end{array} \right)$ (one single additional vector).

4.2. Optimization of the algorithm

Two parameters have been introduced in our strategy. The first one is the stopping criterion of the conjugate gradient, ν_{CG} (the CG iterations are stopped when $\|\underline{\mathbf{R}} - \underline{\underline{\mathbf{K}}}_{\mathrm{T}}\, \underline{\boldsymbol{\Delta \mathbf{U}}}\|_2 / \|\underline{\mathbf{R}}\|_2 \leq \nu_{\mathrm{CG}}$), and the second one is the desired normalised residual ν_{New} for the full nonlinear problem. A parametric study, which is note described here, has shown that an optimal setting is obtained when $\nu_{\mathrm{CG}} = \nu_{\mathrm{New}}$.

5. Results

5.1. Error

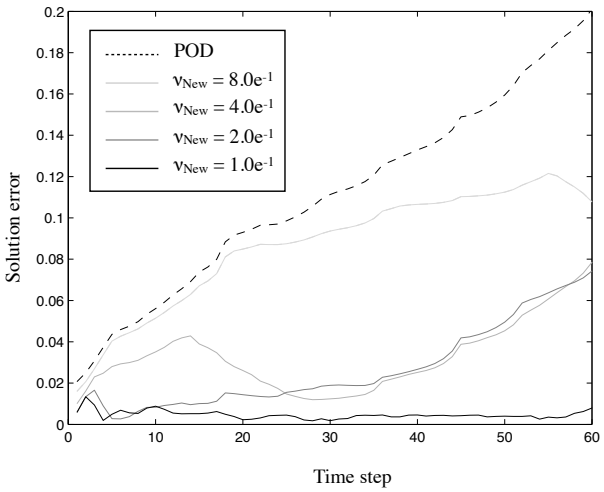

Figure 3. Error for different values of the residual error of the initial problem ν_{New}

The solution error is represented as a function of time on Figure (3), for different value of the residual error threshold $\nu_{\text{New}} = \nu_{\text{CG}}$. The solution obtained converges to the reference solution when ν_{New} decreases. An acceptable representation of the damage state can be obtained with very few iterations of the conjugate gradients ($\nu_{\text{New}} = 4.0e^{-1}$ on Figure (1), which requires only 229 iterations of the conjugate gradients, for 323 iterations of the Newton algorithms). Obviously, the accurate representation of the crack itself requires the fine resolution of the initial problem. However, the cheap results obtained here can be extremely useful if one wants to obtain the long-range effects due the changes in structure's topology, and continue with a model order reduction after its propagation.

5.2. Numerical costs

As shown in the following table, our algorithm does not increase significantly the number of Newton iterations required to achieve convergence and that the additional costs required by the enrichment (due to the conjugate gradient iterations) is relatively low. Indeed, the cost of a conjugate gradient iteration is small campared to the assembly of the linearized stiffness of the reduced problem.

	Newton Iterations	**CG iterations**
POD	345	0
$\nu_{New} = \nu_{CG} = 0.8$	329	83
$\nu_{New} = \nu_{CG} = 0.4$	323	229
$\nu_{New} = \nu_{CG} = 0.2$	341	431
$\nu_{New} = \nu_{CG} = 0.1$	397	897

6. Conclusion

We derived a POD-Krylov model order reduction strategy which permits to control, at low additional costs, the global residual of the nonlinear initial problem by enriching the reduced basis. Our next step concerning the optimization and enhancement of this algorithm is to use the information generated by the Krylov solver to enrich the reduced basis with additional relevant Ritz vectors and to increase the convergence rate of the successive conjugate gradient solves.

We have demonstrated that the method can potentially reproduce the long-range effects of a localized strong evolution of the structure, such as damage evolution, which is a step towards the extension of the applicability of model order reduction strategies to such complex problems.

References

[1] O. Allix and A. Corigliano. Modeling and simulation of crack propagation in mixed-modes interlaminar fracture specimens. *International Journal of Fracture*, 77:11–140, 1996.

[2] O. Allix, P. Kerfriden, and P. Gosselet. On the control of the load increments for a proper description of multiple delamination in a domain decomposition framework. *International Journal for Numerical Methods in Engineering*, DOI:10.1002/nme.2884, 2010.

[3] S. Bordas and B. Moran. Enriched finite elements and level sets for damage tolerance assessment of complex structures. *Engineering Fracture Mechanics*, 73(9):1176–1201, 2006.

[4] F. Chinesta, A. Ammar, and E. Cueto. Proper generalized decomposition of multiscale models. *International Journal for Numerical Methods in Engineering*, DOI:10.1002/nme.2794, 2009.

[5] Z. Dostál. Conjugate gradient method with preconditioning by projector. *International Journal of Computer Mathematics*, 23(3):315–323, 1988.

[6] F. Feyel and J.-L. Chaboche. FE^2 multiscale approach for modelling the elastoviscoplastic behaviour of long fibre SiC/Ti composite materials. *Computer Methods in Applied Mechanics and Engineering*, 183:309–330, 2000.

[7] J. Fish, K. Shek, M. Pandheeradi, and M. S. Shephard. Computational plasticity for composite structures based on mathematical homogenization: Theory and practice. *Computer Methods in Applied Mechanics and Engineering*, 148:53–73, 1997.

[8] G. Franceschini, D. Bigoni, P. Regitnig, and GA Holzapfel. Brain tissue deforms similarly to filled elastomers and follows consolidation theory. *Journal of the Mechanics and Physics of Solids*, 54(12):2592–2620, 2006.

[9] P. Gosselet and C. Rey. Non-overlapping domain decomposition methods in structural mechanics. *Archives of Computational Methods in Engineering*, 13:515–572, 2006.

[10] AD Jefferson and T. Bennett. A model for cementitious composite materials based on micro-mechanical solutions and damage-contact theory. *Computers & Structures*, doi:10.1016/j.compstruc.2008.09.006, 2009.

[11] K. Karhunen. Über lineare methoden in der wahrscheinlichkeitsrechnung. *Annales Academiæ Scientiarum Fennicæ Series A1, Mathematical Physics 37*, 37:1–79, 1947.

[12] P. Kerfriden, O. Allix, and P. Gosselet. A three-scale domain decomposition method for the 3D analysis of debonding in laminates. *Computational Mechanics*, 44(3):343–362, 2009.

[13] P. Ladevèze, J.C. Passieux, and D. Néron. The latin multiscale computational method and the proper generalized decomposition. *Computer Methods in Applied Mechanics and Engineering*, 199(21):1287–1296, 2009.

[14] J. Lemaître and J.-L. Chaboche. *Mechanics of Solid Materials*. Cambridge University Press, 1990.

[15] Y. C. Liang, H. P. Lee, S. P. Lim, W. Z. Lin, K. H. Lee, and C. G. Wu. Proper orthogonal decomposition and its applications - part I: theory. *Journal of Sound and Vibration*, 252(3):527–544, 2002.

[16] M. Loeve. *Probability Theory*. 3rd edition Van Nostrand, Princeton, 1963.

[17] G. Lubineau, P. Ladevèze, and D. Marsal. Towards a bridge between the micro- and mesomechanics of delamination for laminated composites. *Composites Science and Technology*, 66(6):698–712, 2007.

[18] R. Markovinovic and J.D. Jansen. Accelerating iterative solution methods using reduced-order models as solution predictors. *International Journal for numerical Methods in Engineering*, 68:525–54, 2006.

[19] S. Niroomandi, I. Alfaro, E. Cueto, and F. Chinesta. Real-time deformable models of non-linear tissues by model reduction techniques. *Computer Methods and Programs in Biomedicine*, 91(3):223–231, 2008.

[20] J. Pebrel, C. Rey, and P. Gosselet. A nonlinear dual domain decomposition method: application to structural problems with damage. *International Journal for Multiscale Computational Engineering*, 6(3), 2008.

[21] F. Risler and C. Rey. Iterative accelerating algorithms with krylov subspaces for the solution to large-scale nonlinear problems. *Numerical algorithms*, 23:1–30, 2000.

[22] D. Ryckelynck. A priori hyperreduction method: an adaptive approach. *Journal of Computational Physics*, 202(1):346–366, 2005.

[23] D. Ryckelynck. Hyper-reduction of mechanical models involving internal variables. *International Journal for Numerical Methods in Engineering*, 77(1):75 – 89, 2008.

[24] D. Ryckelynck and D. M. Benziane. Multi-level a priori hyper-reduction of mechanical models involving internal variables. *Computer Methods in Applied Mechanics and Engineering*, 199(17-20):1134–1142, 2010.

[25] L. Sirovich. Turbulence and the dynamics of coherent structures. part I: coherent structures. *Quarterly of Applied Mathematics*, 45:561–571, 1987.